Evaluating the E3SM Land Model at a temperate forest site using flux and soil water measurements

Junyi Liang[1,*], Gangsheng Wang[1,*], Daniel M. Ricciuto[1], Lianhong Gu[1], Paul J. Hanson[1], Jeffrey D. Wood[2], Melanie A. Mayes[1]

[1]Environmental Sciences Division & Climate Change Science Institute, Oak Ridge National Laboratory
[2] School of Natural Resources, University of Missouri, Columbia, Missouri, USA

Correspondence to: Junyi Liang (email: liangj@ornl.gov) and Gangsheng Wang (email: wangg@ornl.gov)

Notice: This manuscript has been authored by UT-Battelle, LLC under Contract No. DE-AC05-00OR22725 with the U.S. Department of Energy. The United States Government retains and the publisher, by accepting the article for publication, acknowledges that the United States Government retains a non-exclusive, paid-up, irrevocable, worldwide license to publish or reproduce the published form of this manuscript, or allow others to do so, for United States Government purposes. The Department of Energy will provide public access to these results of federally sponsored research in accordance with the DOE Public Access Plan (http://energy.gov/downloads/doe-public-access-plan).

Abstract. Accurate simulations of soil respiration and carbon dioxide (CO_2) efflux are critical to project global biogeochemical cycles and the magnitude of carbon (C) feedbacks to climate change in Earth system models (ESMs). Currently, soil respiration is not represented well in ESMs, and few studies have attempted to address this deficiency. In this study, we evaluated the simulation of soil respiration in the Energy Exascale Earth System Model (E3SM) using long-term observations from the Missouri Ozark AmeriFlux (MOFLUX) forest site in the central U.S. Simulations using the default model parameters significantly underestimated annual soil respiration and gross primary production, while underestimating soil water potential during growing seasons and overestimating it during non-growing seasons. A site-specific soil water retention curve significantly improved modelled soil water potential, gross primary production and soil respiration. However, the model continued to underestimate soil respiration during peak growing seasons, and overestimate soil respiration during non-peak growing seasons. One potential reason may be that the current model does not adequately represent the seasonal cycle of microbial organisms and soil macroinvertebrates, which have high biomass and activity during peak growing seasons and tend to be dormant during non-growing seasons. Our results confirm that modelling soil respiration can be significantly improved by better model representations of the soil water retention curve.

1 Introduction

Globally, soils store over twice as much carbon (C) as the atmosphere (Chapin III et al., 2011). Soil respiration (SR) is the second largest C flux between terrestrial ecosystems and the atmosphere (Luo and Zhou, 2006). An accurate simulation of SR is critical for projecting terrestrial C status, and therefore climate change, in Earth system models (ESMs) (IPCC, 2013). Despite significant experimental data accumulation and model development during the past decades, simulations of soil CO_2

efflux to the atmosphere still have a high degree of uncertainty (Friedlingstein et al., 2006; Jones et al., 2013; Todd-Brown et al., 2013; Todd-Brown et al., 2014; Tian et al., 2015), calling for comprehensive assessments of model performance against observational data.

To assess the performance of ESMs, different types of data can be used. For example, using atmospheric CO_2
5   measurements, eddy covariance measurements and remote sensing images, Randerson et al. (2009) found that two ESMs underestimated net C uptake during the growing season in temperate and boreal forest ecosystems, primarily due to the delays in the timing of maximum leaf area in the models. By comparing remote sensing estimations from the Moderate Resolution Imaging Spectroradiometer and flux tower datasets, Xia et al. (2017) found that better representations of processes controlling monthly maximum gross primary productivity (GPP) and vegetation C use efficiency (CUE) improved
10   the ability of models to predict the C cycle in permafrost regions.

Despite the significance of large global SR fluxes, SR has rarely been evaluated in ESMs using long-term observations. Among the factors that influence SR, soil water potential (SWP) provides a unified measure of the energy state of soil water that limits the growth and respiration of plants and microbes. Unlike soil temperature (ST) or soil volumetric water content (VWC), however, SWP is difficult to directly monitor in the field. Accurate estimation of SWP largely relies on the soil
15   water retention curve (i.e., the relationship between VWC and SWP), which is highly specific to soil properties (Childs, 1940; Clapp and Hornberger, 1978; Cosby et al., 1984; Tuller and Or, 2004; Moyano et al., 2013). Site-level data have been used to evaluate model representations of other processes, such as phenology, net primary production (NPP), transpiration, leaf area index (LAI), water use efficiency, and nitrogen use efficiency (Richardson et al., 2012; De Kauwe et al., 2013; Walker et al., 2014; Zaehle et al., 2014; Mao et al., 2016; Duarte et al., 2017; Montané et al., 2017). In Powell et al. (2013),
20   the only aspect concerning SR was the sensitivity of SR to VWC in an Amazon forest, but the study resulted in no improvements to simulated SR. Here, we focus on improving simulations by using site-specific measurements to assess multiple factors influencing SR.

We will evaluate the simulation of SR step by step. We assessed underlying mechanisms in the Energy Exascale Earth System Model (E3SM) by using intensive observations at the Missouri Ozark AmeriFlux (MOFLUX) forest site in the
25   central U.S. We first evaluated the effects of two abiotic factors, ST and SWP, on the simulation of SR. Then we evaluated the effects of biotic factors, such as GPP, LAI and Q_{10} of heterotrophic respiration, on the simulation of surface CO_2 efflux to the atmosphere.

2 Materials and Methods

2.1 Study site and measurements

30   The MOFLUX site is located in the University of Missouri's Thomas H. Baskett Wildlife Research and Education Area (latitude 38º44'39"N, longitude 92º12'W). The mean annual precipitation is 1083 mm, while minimum and maximum monthly mean temperatures are −1.3 ℃ (January) and 25.2 ℃ (July), respectively. The site is a temperate, upland oak-

hickory forest, with major tree species consisting of white oak (*Quercus alba* L.), black oak (*Q. velutina* Lam.), shagbark hickory (*Carya ovata* (Mill.) K. Koch), sugar maple (*Acer saccharum* Marsh.), and eastern red cedar (*Juniperus virginiana* L.) (Gu et al., 2016; Wood et al., 2017). The dominant soils are the Weller silt loam and the Clinkenbeard very flaggy clay loam (Young et al., 2001).

5   Ecosystem C, water and energy fluxes, SR, LAI and supporting meteorological measurements were initiated in June 2004 (Gu et al., 2016). Soil respiration was measured within the ecosystem flux footprint using non-flow through non-steady state auto-chambers. From 2004 through 2013, SR was measured using eight automated, custom-built, chambers (ED system; Edwards and Riggs, 2003; Gu et al., 2008) coupled with an infrared gas analyzer (LI-820 Li-Cor Inc., Lincoln, Nebraska). In 2013, this system was replaced with 16 auto-chambers operated using the closed-path system (model LI-8100;

10   Li-Cor Inc., Lincoln, Nebraska). The two systems (ED and Li-8100) were operated side-by-side for several weeks in 2010 and found to produce comparable responses (Paul Hanson, personal communication). Half-hourly SR time series were generated to coincide with the ecosystem flux data set by averaging those chambers sampled in the corresponding averaging period. Net ecosystem CO_2 exchange (NEE) was measured on a 32-m walk-up scaffold tower (Gu et al., 2016). A soil temperature profile sensor (model STP01, HuksefluxUSA, Inc., Center Moriches, NY) measured at 5 depths down to 0.5 m.

15   Soil VWC was measured using water content reflectometers (model CS616, Campbell Scientific Inc., Logan UT) installed beneath each soil chamber. All the data were recorded at half-hourly intervals, which were integrated over time to obtain daily and annual fluxes.

2.2 Ecosystem C flux partitioning

Flux-tower GPP was estimated from measured NEE. To reduce biases resulting from individual methods, three NEE-
20   partitioning approaches were employed. The average and variation of the three methods were used to evaluate the model-simulated GPP. In the first two methods, ecosystem respiration (ER) was estimated from nighttime NEE and extrapolated to daytime, and daytime GPP was calculated from NEE and the extrapolated ER (Reichstein et al., 2005). The only difference between the two methods was whether to exclude night-time data under non-turbulent conditions. In the third method, GPP was estimated by fitting the light-response curve between NEE and radiation (Lasslop et al., 2010). All the partitioning
25   calculations were conducted using the R package *REddyProc* (Reichstein et al., 2017).

2.3 Model description

The E3SM includes coupled carbon and nitrogen cycles, with 10 belowground layers in the biogeochemical module. The land model of E3SM was developed from Community Land Model (CLM 4.5) (Oleson et al., 2013). We implemented off-line E3SM Land Model (ELM) simulations with the CLM-CN soil decomposition module (Thornton and Rosenbloom, 2005;
30   Bonan et al., 2013). In the model, SR was calculated by different CO_2 emission components (Oleson et al., 2013):

$$SR = R_A + R_H \qquad \text{Eq. (1)}$$

$$R_A = R_M + R_G \qquad \text{Eq. (2)}$$

$$R_M = R_{livecroot} + R_{froot} \qquad\qquad \text{Eq. (3)}$$

$$R_{liveroot} = [N]_{livecroot} R_{base} R_{q10}^{(T_{2m}-20)/10} \qquad\qquad \text{Eq. (4)}$$

$$R_{froot} = \sum_{j=1}^{10} [N]_{froot} rootfr_j R_{base} R_{q10}^{(T_{2m}-20)/10} \qquad\qquad \text{Eq. (5)}$$

$$R_G = 0.3 C_{new\_root} \qquad\qquad \text{Eq. (6)}$$

$$R_H = \sum_{j=1}^{10} \sum_{i=1}^{4} SOC_{ij} k_i rf_i \xi_T \xi_W \xi_O \xi_D \xi_N \qquad\qquad \text{Eq. (7)}$$

where R_A and R_H are belowground autotrophic and heterotrophic respiration, respectively. R_A is the sum of root maintenance (R_M) and growth respiration (R_G). $R_{livecroot}$ and R_{froot} are maintenance respiration of live course root and fine root. $[N]_{livecroot}$ and $[N]_{froot}$ are nitrogen content of live coarse and fine roots. R_{base} is the base maintenance respiration at 20 ℃. R_{q10} which equals 2, is the temperature sensitivity of maintenance respiration. T_{2m} is the air temperature at 2 m. C_{new_root} is the new root growth C. R_H is the sum of heterotrophic respiration of four SOC pools with different turnover rates (Oleson et al., 2013) in the 10 soil layers. The parameters k_i and rf_i are the turnover rate and respiration fraction of the ith pool. ξ_T, ξ_W, ξ_O, ξ_D, ξ_N are environmental modifiers of soil temperature, soil water content, oxygen, depth and nitrogen for each layer, respectively. A detailed description of the environmental modification can be found in Oleson et al. (2013). Briefly, the temperature and water modifiers were:

$$\xi_T = Q_{10}^{\left(\frac{T_{soil}-T_{ref}}{10}\right)} \qquad\qquad \text{Eq. (8)}$$

$$\xi_W = \begin{cases} 0 & for\ \Psi < \Psi_{min} \\ \dfrac{log(\Psi_{min}/\Psi_m)}{log(\Psi_{min}/\Psi_s)} & for\ \Psi_{min} \le \Psi \le \Psi_{max} \\ 1 & for\ \Psi > \Psi_{max} \end{cases} \qquad \text{Eq. (9)}$$

where Q_{10} is the temperature sensitivity (the default value is 1.5), T_{ref} is the reference temperature (25 ℃). Ψ_m is the matric water potential, Ψ_{min} is the lower limit for matric potential, and Ψ_s is the matric water potential under saturated conditions.

The E3SM is a grid-based ESM. To assess it using site-level observations, we used a point-run framework which allows the model to simulate individual sites (Mao et al., 2016). With site-specific forcing, a 200-year accelerated decomposition spin-up was performed, followed by a 200-year normal spin-up, before the transient simulation was performed from 1850 to 2013. The vegetation was set as 100% temperate deciduous forest.

2.4 Soil water retention curve

Soil water potential values for the Weller soils (https://soilseries.sc.egov.usda.gov/OSD_Docs/W/WELLER.html) were estimated from observed VWC and soil water retention curves that were developed for the site. To derive the soil water retention curves, soil samples were collected in the area of the flux tower base at two depths: 0 to 30 cm and below 30 cm.

Samples were evaluated periodically for soil water potential using a dewpoint potentiometer (Decagon Devices, Model WP4C) as they dried over time (Hanson et al., 2003).

In the E3SM, the SWP was calculated from VWC based on the Clapp & Hornberger model (Clapp and Hornberger, 1978), in which the SWP-VWC relationship was expressed as

$$\Psi_m = \Psi_s \left(\frac{\theta}{\theta_s}\right)^{-B} \qquad \text{Eq. (10)}$$

where θ and Ψ_m are the VWC and matric potential (MPa); and θ_s and Ψ_s are VWC and matric potential under saturated conditions, and B is a parameter to determine the shape of the SWP-VWC relationship. In the E3SM, all parameters were calculated from the fraction of organic matter (f_{om}), clay content (f_{clay}; %) and sand content (f_{sand}; %) (Cosby et al., 1984; Lawrence and Slater, 2008), where

$$\Psi_s = -\left((1 - f_{om}) \times 10 \times 10^{1.88 - 0.0131 f_{sand}} + 10.3 f_{om}\right) \qquad \text{Eq. (11)}$$

$$\theta_s = \left((1 - f_{om}) \times (0.489 - 0.00126 f_{sand}) + 0.9 f_{om}\right) \qquad \text{Eq. (12)}$$

$$B = (1 - f_{om}) \times (2.91 + 0.159 f_{clay}) + 2.7 f_{om} \qquad \text{Eq. (13)}$$

In addition to the Clapp & Hornberger model, four other empirical models (Brooks and Corey, 1964; van Genuchten, 1980; Fredlund and Xing, 1994; Hanson et al., 2003) were also used to fit the SWP curve against VWC (Table 1, Figure 1).

In the Brooks & Corey model, the SWP-VWC relationship was expressed as

$$\frac{\theta - \theta_r}{\theta_s - \theta_r} = \begin{cases} \left(\frac{\Psi_b}{\Psi_m}\right)^{\lambda} & \Psi_m > \Psi_b \\ 1 & \Psi_m \leq \Psi_b \end{cases} \qquad \text{Eq. (14)}$$

where θ_r and θ_s are the residual and saturated water contents, respectively, θ and Ψ_m are measured VWC and matric potential (MPa), Ψ_b is a parameter related to the soil matric potential at air entry, and λ is related to the soil pore size distribution (Brooks and Corey, 1964).

In the Fredlund & Xing model, the SWP-VWC relationship was described as

$$\frac{\theta - \theta_r}{\theta_s - \theta_r} = \left[\frac{1}{\ln(e + (\Psi_m/a)^n)}\right]^m \qquad \text{Eq. (15)}$$

where a, n and m are parameters determining the shape of the soil water characteristic curve (Fredlund and Xing, 1994).

In the Hanson model (Hanson et al., 2003), soil matric potential was modeled by a double exponential function:

$$\Psi_m = -a^{b\theta^c} - d \qquad \text{Eq. (16)}$$

where a, b, c and d are fitted parameters.

In the van Genuchten model, the SWP-VWC relationship was described as

$$\frac{\theta - \theta_r}{\theta_s - \theta_r} = \left[\frac{1}{1 + (\alpha\Psi_m)^n}\right]^{(1-1/n)} \qquad \text{Eq. (17)}$$

where α (MPa^{-1}) and n are parameters that determine the shape of the soil-water curve (van Genuchten, 1980).

In addition to the default SWP-VWC relationship in the E3SM, all the five empirical models were parameterized using non-linear fitting against measured VWC and SWP data from the study site. The root-mean-square error (RMSE) was used to select the best model representing the SWP-VWC relationship, where smaller RMSE implies a better fit to observational data. The best-fit model was used in two ways. First, it was used to calculate the "observed" SWP from monitored VWC in
5 the field. Second, it was implemented in the E3SM to replace the default SWP model in order to improve the SWP simulation.

2.5 Evaluation of SR in the model

The evaluation of SR was conducted step by step. We first compared observations with the model default output of SR and related factors, including ST, SWP, GPP, and LAI. Thereafter, we attempted to improve the simulation of these factors in
10 order to improve the overall SR simulation by (i) implementing the best-fit SWP-VWC relationship, and (ii) modifying model parameters related to GPP, LAI and SR. GPP-related parameters included the specific leaf area (SLA) at the top of canopy and the fraction of leaf nitrogen in the RuBisCO enzyme. LAI-related parameters included the number of days to complete leaf fall during the end of growing season, the critical day length for senescence (i.e., the length of the day when leaves start to senesce), and a parameter α that was used to produce a linearly-increasing rate of litterfall. In addition, the Q_{10}
15 of heterotrophic respiration was also modified. Because the parameter modification was dependent on the evaluation steps, how the parameters were modified is presented in the Results section.
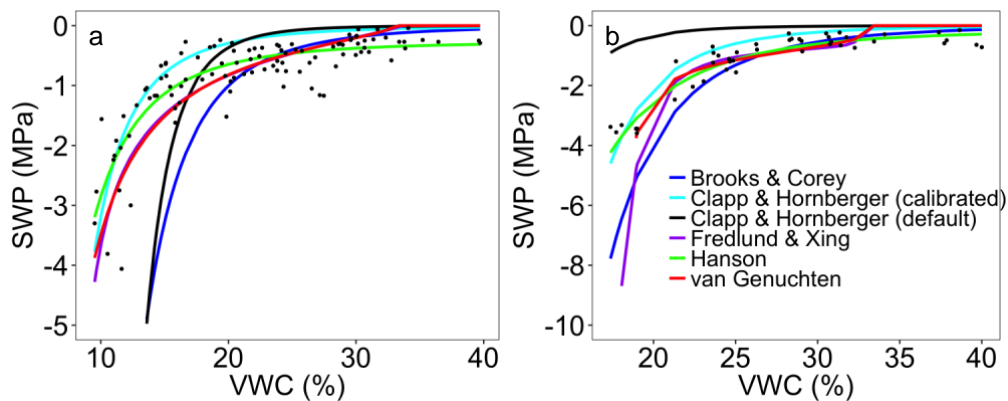
Figure 1: Observed (black dots) and simulated relationship between soil water potential (SWP) and volumetric water content (VWC) by the different models at two soil layers: (a) 0 to 30 cm and (b) below 30 cm.

3 Results

For the upper 30 cm of soil, E3SM simulations using the default Clapp and Hornberger model tended to underestimate the SWP when VWC was less than 15% (Fig. 1a), while SWP rapidly approached zero when VWC was greater than 25% (Fig. 1a). For soil below 30 cm, the E3SM showed a consistent overestimation of SWP when VWC exceeded 15% (Fig. 1b). The

5 default E3SM showed relatively high RMSE for both soil layers, indicating that the SWP-VWC relationship was not well simulated in the E3SM (Table 1). Although the Clapp & Hornberger model performed better by using parameters from non-linear fitting, its performance was not as good as the Hanson and the van Genuchten models (Table 1, Fig. 1). The Hanson model was the best-fit model for the MOFLUX site, showing the smallest RMSE for both soil layers (Table 1, Fig. 1), and was therefore implemented in E3SM to calculate SWP from measured VWC.

10 **Table 1.** Root-mean-square-error (RMSE) of different models in simulating the SWP-VWC relationship for the soil in the MOFLUX site at two depths: 0 to 30 cm and below 30 cm.

Model	< 30 cm	> 30 cm
Clapp & Hornberger (default E3SM)	4.25	1.33
Brooks & Corey	3.91	1.13
Clapp & Hornberger (calibrated)	0.53	0.51
Fredlund & Xing	0.51	2.43
Hanson	0.41	0.34
van Genuchten	0.50	0.36

The E3SM default run significantly underestimated both annual SR and GPP (Fig. 2). In addition, the simulated SR had smaller interannual variability compared to the observations. The model was not able to simulate the steep drop of SR or

15 GPP during the extreme drought in 2012. The simulations of ST and SWP were isolated to analyse their contributions to model performance. Whereas the model simulated ST well at 10 cm depth (Fig. 3a), it tended to underestimate SWP when water is limiting and to overestimate SWP otherwise (Fig. 3b). Implementing the data-constrained Hanson model significantly improved the simulation of SWP, showing a greater R^2 and a much smaller RMSE than that of the default run (Fig. 3b). After improving the simulation of SWP, the model better matched the observed annual SR and GPP (Fig. 2). The

20 mean annual simulations of SR and GPP fell into the 95% confidence interval of observations (red bar in the inserted plot in Fig. 2). In addition, the changes in annual SR and GPP (i.e., the differences between before and after the improved SWP simulation) showed a linear relationship (Fig. 4).
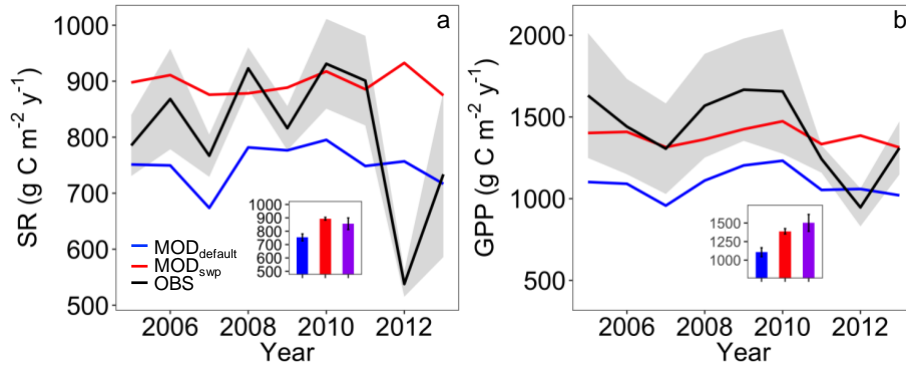
Figure 2: Annual soil respiration (SR) and gross primary production (GPP). Blue and red lines are model outputs before (MOD$_{default}$) and after (MOD$_{swp}$) soil water potential improvement, respectively. Black lines and grey area are the observed (OBS) mean and 95% confidence interval (CI), which were calculated from 8 field replications for SR, and from three different net ecosystem exchange partitioning methods for GPP. The inserted bar plots are mean annual average ± 95% CI across 2005-2011 for MOD$_{default}$ (blue), MOD$_{swp}$ (red) and OBS (purple).
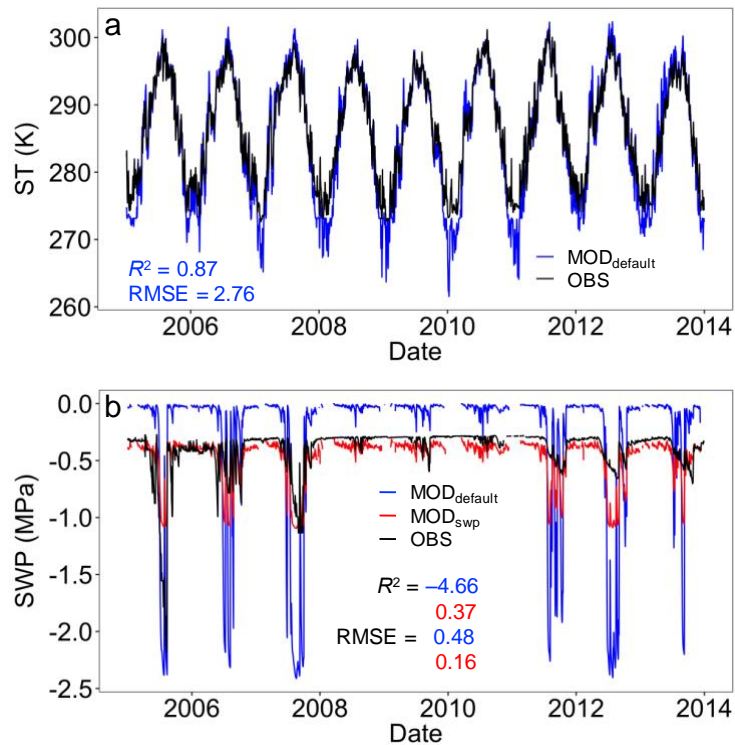
Figure 3: Daily soil temperature (ST) and soil water potential (SWP) at 10 cm. Blue and red lines/dots are model outputs before (MOD$_{default}$) and after (MOD$_{swp}$) soil water potential improvement, respectively. R^2 and RMSE are shown in corresponding colours. Extremely low SWP values due to frozen soil water are not shown.
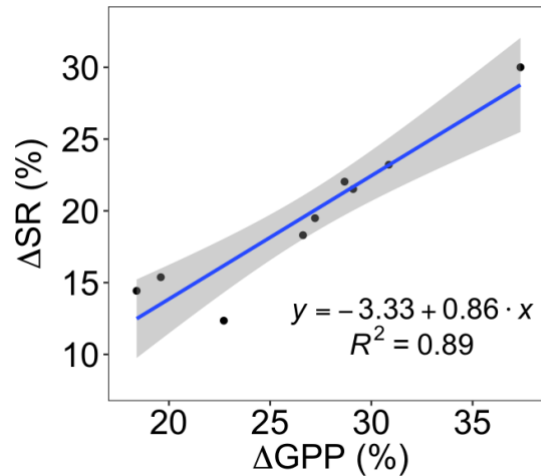
Figure 4: Relationship between changes in simulated annual soil respiration (ΔSR) and gross primary production (ΔGPP) induced by improvement of soil water potential in the model.

Despite the improved simulation of SR, the model still underestimated SR and GPP during peak growing seasons when SR and GPP were high, but overestimated them during non-peak growing seasons (Figs. 5, Fig. S1). In other words, though the improved simulation of SWP increased SR and GPP during peak growing seasons, the model still showed systematic errors (Fig. 5). We attempted to improve the seasonal simulations of SR, GPP and LAI by modifying several related parameters (Table 2). Using measurements of NEE, maximum LAI and latent heat fluxes from the MOFLUX site, Lu et al. (unpublished) calibrated a polynomial surrogate model of CLM4.5. Based on their results, we modified two parameters, i.e., the SLA at the canopy top from 0.03 to 0.01, and the fraction of leaf nitrogen in the RuBisCO enzyme from 0.1007 to 0.12.
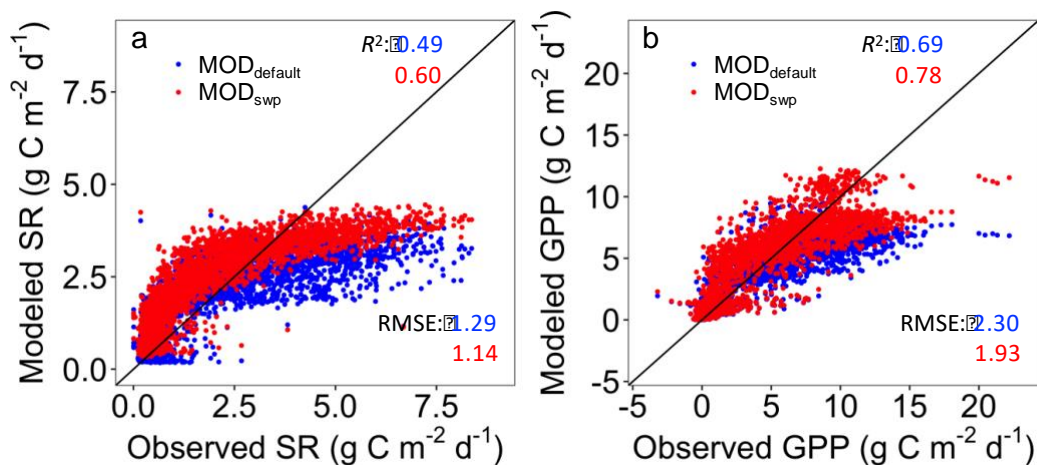
Figure 5: Observed vs. modeled soil respiration (SR) and gross primary production (GPP). Blue and red dots are model outputs before ($MOD_{default}$) and after (MOD_{swp}) soil water potential improvement, respectively. The black line is 1:1 line.

Table 2. Modified parameters to better simulate gross primary production (GPP) and leaf area index (LAI) at the MOFLUX site in the E3SM.

Parameter name (unit*)	Parameter description	Default model value	Tuned values
slatop	Specific leaf area at top of canopy	0.03	0.01
flnr	Fraction of leaf nitrogen in RuBisCO enzyme	0.1007	0.12
ndays_off (d)	Number of days to complete leaf offset	15	45
Crit_dayl (s)	Critical day length for senescence	39300	43200
α	To control the rate coefficient r_{xfer_off} to produce a linearly-increasing litterfall rate	2	10

*$slatop$, $flnr$ and α are unitless

Comparing the simulated LAI with the observations (Fig. 6), we found that the parameter *ndays_off* (number of days to complete leaf offset) in the E3SM was too short (default value = 15 days) for the MOFLUX site. Thus, we reset the value of *ndays_off* to 45 days. We also modified the values of two additional parameters, i.e., *crit_dayl* and α correspondingly (Table 2). Parameter *crit_dayl* (the critical day length for senescence, units: second) triggers the leaf falling during the end of the

10 growing season. Parameter (α) is used to produce a linearly-increasing litter-fall rate. The adjustment of the aforementioned five parameters (Table 2) significantly reduced the LAI to within a more reasonable range, showing an increased R^2 from 0.05 to 0.91 and a reduced RMSE from 1.15 to 0.34 (Fig. 6a). However, the simulation of GPP was not improved, though the simulation during peak growing season was increased (Fig. 6b). The model was still not able to reach the high values of SR observed during peak growing seasons, even when the modeled GPP exceeded the observations (Fig. 6b, c). In addition, the

15 modeled SR during non-peak growing seasons was not improved (Fig. 6c).
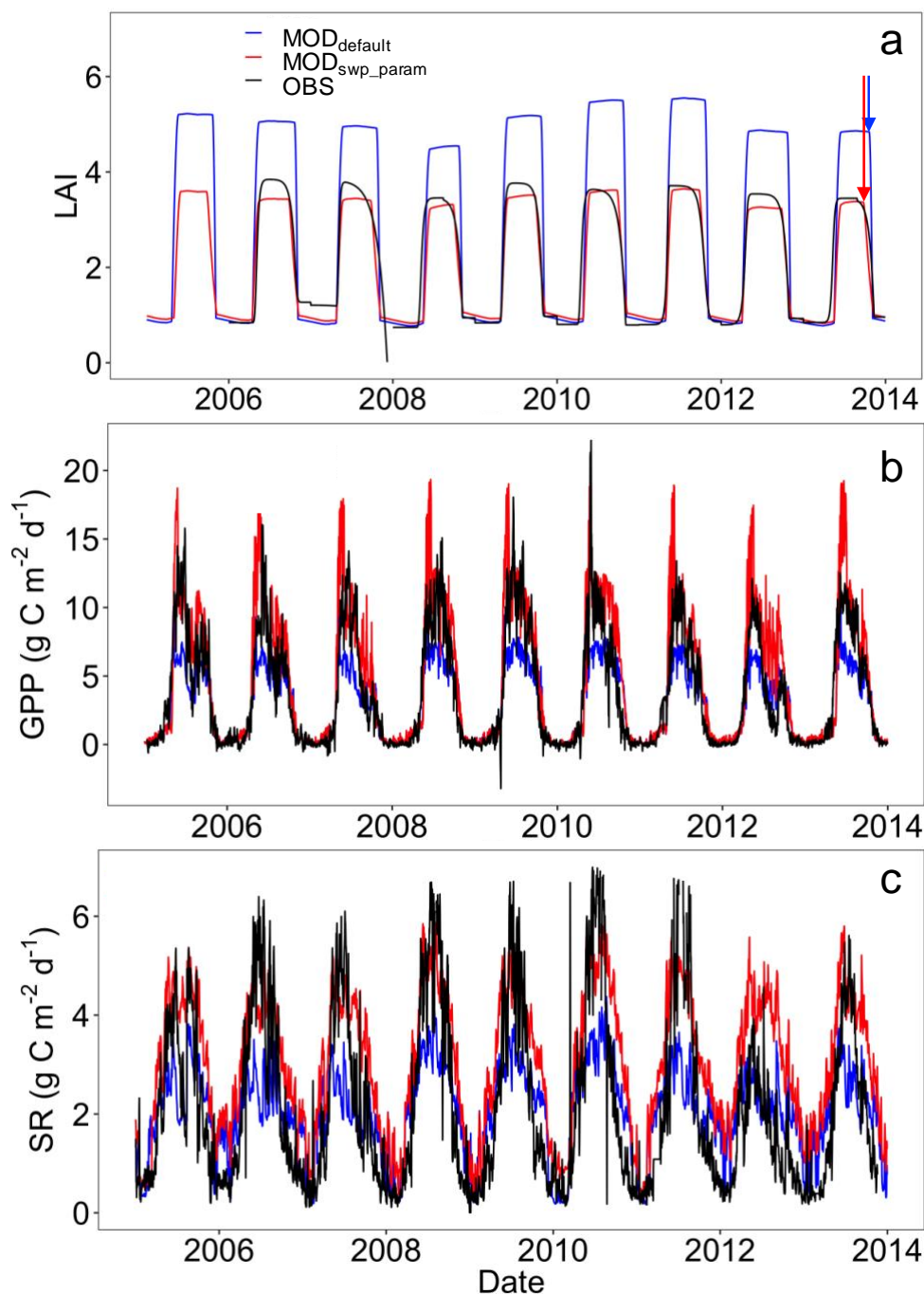
Figure 6 Daily leaf area index (LAI), gross primary production (GPP) and soil respiration (SR). OBS: observation; MOD_default: model output before soil water potential improvement; MOD_swp_param: model output after soil water potential improvement and parameter modification. **a,** the blue (MOD_default) and red (MOD_swp_param) arrows are used to illustrate the earlier start of litterfall in MOD_swp_param.

4 Discussion

4.1 Effect of SWP on annual SR

Constraining the SWP-VWC relationship with site-specific data and using the Hanson model instead of the E3SM default model (Fig. 1) significantly improved the model representation of SWP (Fig. 3). The modeled annual SR in the E3SM was

5 also substantially improved (Fig. 2a). Although SWP can directly affect SR, the improved annual SR simulation was likely due to the indirect influence of SWP on GPP. The land model of E3SM underestimated GPP in this study (Fig. 2b). Similarly, a recent study showed that the CLM4.5 significantly underestimated GPP at a coniferous forest in northeastern United States as well (Duarte et al., 2017). GPP affects the substrate supply for SR, as evidenced by the close relationship between changes in SR and GPP (Fig. 4), which is consistent with experimental evidence showing GPP can directly affect

10 the magnitude of SR (Craine et al., 1999; Högberg et al., 2001; Wan and Luo, 2003; Verburg et al., 2004; Gu et al., 2008). The simulation of SWP in the default E3SM was poor compared with that of ST (Fig. 2), which may be a common issue in ESMs. For example, using a reduced-complexity model, Todd-Brown et al. (2013) demonstrated that the spatial variation in soil C in most ESMs is primarily dependent on C input (i.e., NPP) and ST, showing R^2 values between 0.62 and 0.93 for 9 of 11 ESMs. However, the same reduced-complexity model, driven by observed NPP and ST, can only explain 10% of the

15 variation in the Harmonized World Soil Database observational database (Todd-Brown et al., 2013). These previous results indicate that other important factors affecting soil C dynamics, in addition to NPP and ST, are inadequately simulated in ESMs (Powell et al., 2013; Reyes et al., 2017). Powell et al. (2013) showed that differential sensitivity of SR to VWC in several ESMs using observations in two Amazon forests. Our analyses in this study indicate that improving the modeled SWP can significantly improve SR simulations. Thus, we argue that the SWP simulation in ESMs should be calibrated

20 carefully with observations, and/or by using different model representations of the SWP-VMC relationship.

In this study, we derived better SWP-VWC relationship by using non-linear fitting, primarily because of the availability of soil moisture retention curve data. It is an efficient method when site-level data is available, but it is not realistic to calibrate the water retention curve for every site. The SWP-VWC relationship is dependent on soil texture (Clapp and Hornberger, 1978; Cosby et al., 1984; Tuller and Or, 2004), so building relationships between model parameters and soil

25 texture may allow efficient extrapolations of site-level measurements to regional and global scales.

Parameters in the default Clapp & Hornberger model used in the E3SM were derived from synthesizing data across soil textural classes (Clapp and Hornberger, 1978; Cosby et al., 1984; Lawrence and Slater, 2008). The data were derived from over 1,000 soil samples from 11 USDA soil textural classes (Holtan et al., 1968; Rawls et al., 1976). The dependence of model parameters on soil texture were derived from a regression of these 11 data points, i.e., the mean parameter values of

30 11 soil textural classes against the sand or clay fractions (Cosby et al., 1984). Because no actual sand or clay content of soil samples was reported in the original databases (i.e., only the soil textural classes were reported), the sand and clay fractions used for the regression were obtained from midpoint values of each textural class (Clapp and Hornberger, 1978; Cosby et al., 1984). One potential issue is that soil samples in the same textural classes can have different sand and clay contents and

SWP-VWC relationships, which may not be fully represented when they are grouped together. Consequently, the parameterized Clapp & Hornberger model may still perform poorly for specific sites, e.g., the MOFLUX site. A re-analysis of an updated SWP-VWC database, with actual sand and clay content measurements, may enable improved relationships between model parameters and soil texture in the water retention model.

5   In addition, different empirical models have been developed to describe the SWP-VWC relationship (Brooks and Corey, 1964; Clapp and Hornberger, 1978; van Genuchten, 1980; Fredlund and Xing, 1994; Hanson et al., 2003). These models could be evaluated with an updated SWP-VWC database, and the selected best-fit model(s) could be used to calculate SWP in the field from continuously monitored VWC (e.g., from AmeriFlux network) on different spatial and temporal scales. A new field SWP-VWC database at different scales could be used as a benchmark to improve simulations of soil water and
10   biogeochemical processes in ESMs.

4.2 Improving the representation of seasonal variability of SR

Although the simulation of the SWP improved the representation of both annual SR and GPP, the E3SM continued to underestimate SR during peak growing seasons and overestimate SR during other seasons (Figs. 5, 6c, Fig. S1). Since it has been demonstrated that GPP can directly influence the magnitude of SR (Craine et al., 1999; Högberg et al., 2001; Wan and
15   Luo, 2003; Verburg et al., 2004), the underestimated SR during peak growing seasons may be due to an underestimation of GPP. However, our analyses showed that the modeled SR was not able to reach the observed peak in most years even when the modeled GPP exceeded the observation (Fig. 6). In addition, the parameter modification increased GPP during both peak and non-peak growing seasons, resulting in an even greater overestimation of SR during non-peak growing seasons (Fig. 6). These results suggest that simply increasing GPP may not be adequate to increase the seasonal variability of the simulated
20   SR. Specifically, heterotrophic respiration contributed a majority proportion (i.e., over 85%) to total SR during non-growing seasons (Fig. 7), suggesting that the overestimation of SR during these seasons was primarily due to the biased heterotrophic respiration simulation.

A potential reason for the biased heterotrophic respiration simulation may be related to the temperature sensitivity (Q_{10}). Theoretically, a higher Q_{10} can result in greater seasonal variability of SR (Fig. S2). Compared to relatively small Q_{10} values,
25   a larger Q_{10} can lead to lower heterotrophic respiration when temperature is below the reference temperature, and greater heterotrophic respiration when temperature is above the reference (Fig. S2). In the E3SM, the reference temperature is 25 ℃ and the Q_{10} of heterotrophic respiration is 1.5 (Oleson et al., 2013). A previous study derived a much greater Q_{10} value (i.e., 2.83) when the parameters were calibrated with data from another temperate forest (Mao et al., 2016). We hypothesized that the Q_{10} value of 1.5 may be too small for the MOFLUX site. We arbitrarily increased Q_{10} from 1.5 to 2.5, but there were
30   minimal effects on the SR simulation (Fig. S3). This indicates that modifying the temperature sensitivity of heterotrophic respiration may not improve the modeled representation of seasonality of SR in the E3SM.
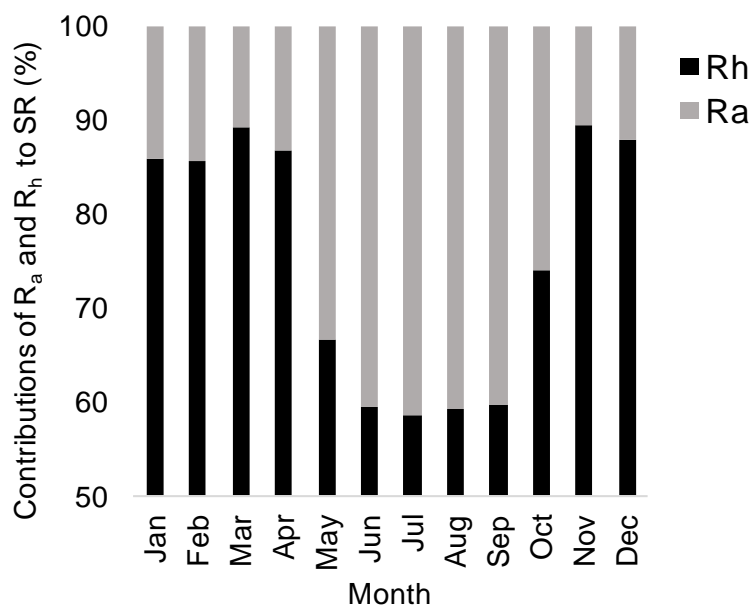
Figure 7: Modelled contributions of autotrophic (R_a) and heterotrophic (R_h) respiration to total soil respiration (SR).

Another potential reason for the biased heterotrophic respiration simulation may be that the seasonality of microbial organisms was not adequately represented in the model. Like most ESMs, the E3SM represents soil C dynamics using linear

5   differential equations and assumes that SR is a substrate-limited process in the model. However, producers of CO_2 in soils, microbial organisms, have a significant seasonal cycle (Lennon and Jones, 2011). These organisms usually have very high biomass and activity during growing season peaks with favorable conditions of temperature, moisture and substrate supply, and tend to be dormant under stressful conditions (Lennon and Jones, 2011; Stolpovsky et al., 2011; Wang et al., 2014; Wang et al., 2015). The seasonality of microbial biomass and activity, in addition to that of GPP and ST, may contribute to

10   the seasonal variability of SR.

Additionally, lacking representation of macroinvertebrate and other forest floor and soil fauna in the E3SM may be another reason. There is a high density of earthworms at the MOFLUX site (Wenk et al., 2016). Earthworms can shred and redistribute soil C and change soil aggregation structure, which may alter soil C dynamics and CO_2 efflux to the atmosphere (Verhoef and Brussaard, 1990; Brussaard et al., 2007; Coleman, 2008). Like microbial organisms, earthworms usually have

15   a significant seasonal cycle, showing high biomass and high activity during peak growing seasons and tending to be dormant during non-growing seasons (Wenk et al., 2016). However, a recent review suggests that current experimental evidence and conceptual understanding remains insufficient to support the development of explicit representation of fauna in ESMs (Grandy et al., 2016). Therefore, data collection focused on seasonal variations in fauna and microbial biomass and activity might enable further improvements in the representation of seasonal variation in SR.

5 Conclusions

In this study, we used temporally extensive and spatially distributed site observations of SR to assess the capabilities of E3SM. These results indicated that an improved representation of SWP within the model provided better simulations of annual SR. This underscores the need to calibrate SWP in ESMs for more accurate projections of coupled climate and

5   biogeochemical cycles. Notwithstanding this improvement, however, the E3SM still underestimated the magnitude of SR during the peak growing season and overestimated SR during the non-peak growing season. Additional adjustments of driving variables for SR, including GPP, LAI and the Q_{10} of heterotrophic respiration did not improve the model prediction. It may be that inadequate model representation of the seasonality of fauna and microbial organisms could be explored as means to achieve better fit. Future incorporation of explicit microbial processes with relevant data collection activities may

10   therefore enable improved model simulations.

Code availability. The code for E3SM is available at https://github.com/ACME-Climate.

Data availability. The data for this paper are available upon request to the corresponding author.

Competing interests. The authors declare that they have no conflict of interest.

Acknowledgements. Authors thank Dan Lu for sharing unpublished data and constructive comments. This work is financially

15   supported by the U.S. Department of Energy (DOE) Office of Biological and Environmental Research through the Terrestrial Ecosystem Science Scientific Focus Area (TES-SFA) at Oak Ridge National Laboratory (ORNL), the Climate Model Development and Validation (CMDV) project and the Energy Exascale Earth System Model (E3SM) project. ORNL is managed by UT-Battelle, LLC, under contract DE-AC05-00OR22725 with the U.S. DOE.

References

20   Bonan, G. B., Hartman, M. D., Parton, W. J., and Wieder, W. R.: Evaluating litter decomposition in earth system models with long-term litterbag experiments: an example using the Community Land Model version 4 (CLM4), Global Change Biology, 19, 957-974, 2013.

Brooks, R. H., and Corey, A. T.: Hydraulic properties of porous media, Hydrology Papers, No. 3, Colorado State university, Fort Collins, Colorado, 1964.

25   Brussaard, L., de Ruiter, P. C., and Brown, G. G.: Soil biodiversity for agricultural sustainability, Agr Ecosyst Environ, 121, 233-244, 2007.

Chapin III, F. S., Matson, P. A., and Vitousek, P.: Principles of terrestrial ecosystem ecology, Springer, 2011.

Childs, E.: The use of soil moisture characteristics in soil studies, Soil Sci, 50, 239-252, 1940.

Clapp, R. B., and Hornberger, G. M.: Empirical Equations for Some Soil Hydraulic-Properties, Water Resour Res, 14, 601-604, 1978.

5   Coleman, D. C.: From peds to paradoxes: Linkages between soil biota and their influences on ecological processes, Soil Biol Biochem, 40, 271-289, 2008.

Cosby, B. J., Hornberger, G. M., Clapp, R. B., and Ginn, T. R.: A Statistical Exploration of the Relationships of Soil-Moisture Characteristics to the Physical-Properties of Soils, Water Resour Res, 20, 682-690, 1984.

Craine, J. M., Wedin, D. A., and Chapin, F. S.: Predominance of ecophysiological controls on soil CO_2 flux in a Minnesota
10   grassland, Plant and Soil, 207, 77-86, 1999.

De Kauwe, M. G., Medlyn, B. E., Zaehle, S., Walker, A. P., Dietze, M. C., Hickler, T., Jain, A. K., Luo, Y. Q., Parton, W. J., Prentice, I. C., Smith, B., Thornton, P. E., Wang, S. S., Wang, Y. P., Warlind, D., Weng, E. S., Crous, K. Y., Ellsworth, D. S., Hanson, P. J., Seok Kim, H., Warren, J. M., Oren, R., and Norby, R. J.: Forest water use and water use efficiency at elevated CO_2: a model-data intercomparison at two contrasting temperate forest FACE sites, Global Change Biology,
15   19, 1759-1779, 2013.

Duarte, H. F., Raczka, B. M., Ricciuto, D. M., Lin, J. C., Koven, C. D., Thornton, P. E., Bowling, D. R., Lai, C. T., Bible, K. J., and Ehleringer, J. R.: Evaluating the Community Land Model (CLM4.5) at a coniferous forest site in northwestern United States using flux and carbon-isotope measurements, Biogeosciences, 14, 4315-4340, 2017.

Edwards, N. T., and Riggs, J. S.: Automated monitoring of soil respiration: A moving chamber design, Soil Sci Soc Am J,
20   67, 1266-1271, 2003.

Fredlund, D. G., and Xing, A. Q.: Equations for the Soil-Water Characteristic Curve, Can Geotech J, 31, 521-532, 1994.

Friedlingstein, P., Cox, P., Betts, R., Bopp, L., Bloh, W. v., Brovkin, V., Cadule, P., Doney, S., Eby, M., Fung, I., Bala, G., John, J., Jones, C., Joos, F., Kato, T., Kawamiya, M., Knorr, W., Lindsay, K., Matthews, H. D., Raddatz, T., Rayner, P., Reick, C., Roeckner, E., Schnitzler, K.-G., Schnur, R., Strassmann, K., Weaver, A. J., Yoshikawa, C., and Zeng, N.:
25   Climate–Carbon Cycle Feedback Analysis: Results from the C4MIP Model Intercomparison, Journal of Climate, 19, 3337-3353, 10.1175/jcli3800.1, 2006.

Grandy, A. S., Wieder, W. R., Wickings, K., and Kyker-Snowman, E.: Beyond microbes: Are fauna the next frontier in soil biogeochemical models?, Soil Biol Biochem, 102, 40-44, 2016.

Gu, L., Hanson, P. J., Mac Post, W., and Liu, Q.: A novel approach for identifying the true temperature sensitivity from soil
30   respiration measurements, Global Biogeochem Cy, 22, 10.1029/2007GB003164, 2008.

Gu, L. H., Pallardy, S. G., Yang, B., Hosman, K. P., Mao, J. F., Ricciuto, D., Shi, X. Y., and Sun, Y.: Testing a land model in ecosystem functional space via a comparison of observed and modeled ecosystem flux responses to precipitation regimes and associated stresses in a Central US forest, J Geophys Res-Biogeo, 121, 1884-1902, 2016.

Hanson, P. J., O'Neill, E. G., Chambers, M. L. S., Riggs, J. S., Joslin, J. D., and Wolfe, M. H.: Soil respiration and litter
decomposition, in: North American temperate deciduous forest responses to changing precipitation regimes, Springer,
163-189, 2003.

Högberg, P., Nordgren, A., Buchmann, N., Taylor, A. F. S., Ekblad, A., Hogberg, M. N., Nyberg, G., Ottosson-Lofvenius,
M., and Read, D. J.: Large-scale forest girdling shows that current photosynthesis drives soil respiration, Nature, 411,
789-792, 2001.

Holtan, H. N., England, C. B., Lawless, G. P., and Schumaker, G. A.: Moisture-tension data for selected soils on
experimental watersheds, 609 pp., 1968.

IPCC: Climate Change 2013: The Physical Science Basis. Contribution of Working Group I to the Fifth Assessment Report
of the Intergovernmental Panel on Climate Change, Cambridge University Press, Cambridge, United Kingdom and New
York, NY, USA, 2013.

Jones, C., Robertson, E., Arora, V., Friedlingstein, P., Shevliakova, E., Bopp, L., Brovkin, V., Hajima, T., Kato, E.,
Kawamiya, M., Liddicoat, S., Lindsay, K., Reick, C. H., Roelandt, C., Segschneider, J., and Tjiputra, J.: Twenty-First-
Century Compatible CO_2 Emissions and Airborne Fraction Simulated by CMIP5 Earth System Models under Four
Representative Concentration Pathways, Journal of Climate, 26, 4398-4413, 10.1175/jcli-d-12-00554.1, 2013.

Lasslop, G., Reichstein, M., Papale, D., Richardson, A. D., Arneth, A., Barr, A., Stoy, P., and Wohlfahrt, G.: Separation of
net ecosystem exchange into assimilation and respiration using a light response curve approach: critical issues and
global evaluation, Global Change Biology, 16, 187-208, 10.1111/j.1365-2486.2009.02041.x, 2010.

Lawrence, D. M., and Slater, A. G.: Incorporating organic soil into a global climate model, Clim Dynam, 30, 145-160, 2008.

Lennon, J. T., and Jones, S. E.: Microbial seed banks: the ecological and evolutionary implications of dormancy, Nature
reviews. Microbiology, 9, 119, 2011.

Luo, Y., and Zhou, X.: Soil respiration and the environment, Academic press, 2006.

Mao, J., Ricciuto, D. M., Thornton, P. E., Warren, J. M., King, A. W., Shi, X., Iversen, C. M., and Norby, R. J.: Evaluating
the Community Land Model in a pine stand with shading manipulations and $^{13}CO_2$ labeling, Biogeosciences, 13, 641-
657, 2016.

Montané, F., Fox, A. M., Arellano, A. F., MacBean, N., Alexander, M. R., Dye, A., Bishop, D. A., Trouet, V., Babst, F., and
Hessl, A. E.: Evaluating the effect of alternative carbon allocation schemes in a land surface model (CLM4. 5) on
carbon fluxes, pools, and turnover in temperate forests, Geosci Model Dev, 10, 3499-3517, 2017.

Moyano, F. E., Manzoni, S., and Chenu, C.: Responses of soil heterotrophic respiration to moisture availability: An
exploration of processes and models, Soil Biol Biochem, 59, 72-85, 2013.

Oleson, K. W., Lawrence, D. M., Bonan, G. B., Drewniak, B., Huang, M., Koven, C. D., Levis, S., Li, F., Riley, W. J.,
Subin, Z. M., Swenson, S., Thornton, P. E., Bozbiyik, A., R., F., Heald, C. L., Kluzek, E., Lamarque, J. F., Lawrence, P.
J., Leung, L. R., Lipscomb, W., Muszala, S. P., Ricciuto, D. M., Sacks, W. J., Sun, Y., Tang, J., and Yang, Z. L.:

Technical Description of Version 4.5 of the Community Land Model (CLM), NCAR Technical Note NCAR/TN-503+ STR, Boulder, Colorado, 2013.

Powell, T. L., Galbraith, D. R., Christoffersen, B. O., Harper, A., Imbuzeiro, H. M. A., Rowland, L., Almeida, S., Brando, P. M., da Costa, A. C. L., Costa, M. H., Levine, N. M., Malhi, Y., Saleska, S. R., Sotta, E., Williams, M., Meir, P., and Moorcroft, P. R.: Confronting model predictions of carbon fluxes with measurements of Amazon forests subjected to experimental drought, New Phytologist, 200, 350-364, 2013.

Randerson, J. T., Hoffman, F. M., Thornton, P. E., Mahowald, N. M., Lindsay, K., Lee, Y. H., Nevison, C. D., Doney, S. C., Bonan, G., Stockli, R., Covey, C., Running, S. W., and Fung, I. Y.: Systematic assessment of terrestrial biogeochemistry in coupled climate-carbon models, Global Change Biology, 15, 2462-2484, 2009.

Rawls, W., Yates, P., and Asmussen, L.: Calibration of selected infiltration equations for the Georgia Coastal Plain, Report ARS-S-113 July 1976. 110 p, 2 fig, 8 tab, 25 ref, 1 append., 1976.

Reichstein, M., Falge, E., Baldocchi, D., Papale, D., Aubinet, M., Berbigier, P., Bernhofer, C., Buchmann, N., Gilmanov, T., Granier, A., Gr??nwald, T., Havr??nkov, K., Ilvesniemi, H., Janous, D., Knohl, A., Laurila, T., Lohila, A., Loustau, D., Matteucci, G., Meyers, T., Miglietta, F., Ourcival, J. M., Pumpanen, J., Rambal, S., Rotenberg, E., Sanz, M., Tenhunen, J., Seufert, G. n., Vaccari, F., Vesala, T., Yakir, D., and Valentini, R.: On the separation of net ecosystem exchange into assimilation and ecosystem respiration: Review and improved algorithm, Global Change Biology, 11, 1424-1439, 10.1111/j.1365-2486.2005.001002.x, 2005.

Reichstein, M., Moffat, A. M., Wutzler, T., and Sickel, K.: REddyProc: Data processing and plotting utilities of (half-)hourly eddy-covariance measurements. R package version 1.0.0/r18. https://r-forge.r-project.org/projects/reddyproc/, 2017.

Reyes, W. M., Epstein, H. E., Li, X., McGlynn, B. L., Riveros-Iregui, D. A., and Emanuel, R. E.: Complex terrain influences ecosystem carbon responses to temperature and precipitation, Global Biogeochem Cy, 31, 1306-1317, 10.1002/2017GB005658, 2017.

Richardson, A. D., Anderson, R. S., Arain, M. A., Barr, A. G., Bohrer, G., Chen, G. S., Chen, J. M., Ciais, P., Davis, K. J., Desai, A. R., Dietze, M. C., Dragoni, D., Garrity, S. R., Gough, C. M., Grant, R., Hollinger, D. Y., Margolis, H. A., McCaughey, H., Migliavacca, M., Monson, R. K., Munger, J. W., Poulter, B., Raczka, B. M., Ricciuto, D. M., Sahoo, A. K., Schaefer, K., Tian, H. Q., Vargas, R., Verbeeck, H., Xiao, J. F., and Xue, Y. K.: Terrestrial biosphere models need better representation of vegetation phenology: results from the North American Carbon Program Site Synthesis, Global Change Biology, 18, 566-584, 2012.

Stolpovsky, K., Martinez-Lavanchy, P., Heipieper, H. J., Van Cappellen, P., and Thullner, M.: Incorporating dormancy in dynamic microbial community models, Ecol Model, 222, 3092-3102, 2011.

Thornton, P. E., and Rosenbloom, N. A.: Ecosystem model spin-up: Estimating steady state conditions in a coupled terrestrial carbon and nitrogen cycle model, Ecol Model, 189, 25-48, 2005.

Tian, H. Q., Lu, C. Q., Yang, J., Banger, K., Huntzinger, D. N., Schwalm, C. R., Michalak, A. M., Cook, R., Ciais, P., Hayes, D., Huang, M. Y., Ito, A., Jain, A. K., Lei, H. M., Mao, J. F., Pan, S. F., Post, W. M., Peng, S. S., Poulter, B.,

Ren, W., Ricciuto, D., Schaefer, K., Shi, X. Y., Tao, B., Wang, W. L., Wei, Y. X., Yang, Q. C., Zhang, B. W., and Zeng, N.: Global patterns and controls of soil organic carbon dynamics as simulated by multiple terrestrial biosphere models: Current status and future directions, Global Biogeochem Cy, 29, 775-792, 2015.

Todd-Brown, K., Randerson, J., Post, W., Hoffman, F., Tarnocai, C., Schuur, E., and Allison, S.: Causes of variation in soil carbon simulations from CMIP5 Earth system models and comparison with observations, Biogeosciences, 10, 2013.

Todd-Brown, K. E. O., Randerson, J. T., Hopkins, F., Arora, V., Hajima, T., Jones, C., Shevliakova, E., Tjiputra, J., Volodin, E., Wu, T., Zhang, Q., and Allison, S. D.: Changes in soil organic carbon storage predicted by Earth system models during the 21st century, Biogeosciences, 11, 2341-2356, 10.5194/bg-11-2341-2014, 2014.

Tuller, M., and Or, D.: Retention of water in soil and the soil water characteristic curve, Encyclopedia of Soils in the Environment, 4, 278-289, 2004.

van Genuchten, M. T.: A Closed-Form Equation for Predicting the Hydraulic Conductivity of Unsaturated Soils, Soil Sci Soc Am J, 44, 892-898, 1980.

Verburg, P. S. J., Arnone, J. A., Obrist, D., Schorran, D. E., Evans, R. D., Leroux-Swarthout, D., Johnson, D. W., Luo, Y. Q., and Coleman, J. S.: Net ecosystem carbon exchange in two experimental grassland ecosystems, Global Change Biology, 10, 498-508, 2004.

Verhoef, H. A., and Brussaard, L.: Decomposition and Nitrogen Mineralization in Natural and Agroecosystems - the Contribution of Soil Animals, Biogeochemistry, 11, 175-211, 1990.

Walker, A. P., Hanson, P. J., De Kauwe, M. G., Medlyn, B. E., Zaehle, S., Asao, S., Dietze, M., Hickler, T., Huntingford, C., Iversen, C. M., Jain, A., Lomas, M., Luo, Y. Q., McCarthy, H., Parton, W. J., Prentice, I. C., Thornton, P. E., Wang, S. S., Wang, Y. P., Warlind, D., Weng, E. S., Warren, J. M., Woodward, F. I., Oren, R., and Norby, R. J.: Comprehensive ecosystem model-data synthesis using multiple data sets at two temperate forest free-air CO_2 enrichment experiments: Model performance at ambient CO_2 concentration, J Geophys Res-Biogeo, 119, 937-964, 2014.

Wan, S. Q., and Luo, Y. Q.: Substrate regulation of soil respiration in a tallgrass prairie: Results of a clipping and shading experiment, Global Biogeochem Cy, 17, 2003.

Wang, G., Mayes, M. A., Gu, L., and Schadt, C. W.: Representation of dormant and active microbial dynamics for ecosystem modeling, PloS one, 9, e89252, 2014.

Wang, G., Jagadamma, S., Mayes, M. A., Schadt, C. W., Steinweg, J. M., Gu, L., and Post, W. M.: Microbial dormancy improves development and experimental validation of ecosystem model, The ISME journal, 9, 226, 2015.

Wenk, E. S., Callaham, M. A., O'Brien, J. J., and Hanson, P. J.: Soil Macroinvertebrate Communities across a Productivity Gradient in Deciduous Forests of Eastern North America, Northeast Nat, 23, 25-44, 2016.

Wood, J., Knapp, B. O., Muzika, R.-M., Stambaugh, M. C., and Gu, L.: The importance of drought-pathogen interactions in driving oak mortality events in the Ozark Border Region, Environmental Research Letters, 10.1088/1748-9326/aa94fa, 2017.

Xia, J., McGuire, A. D., Lawrence, D., Burke, E., Chen, G., Chen, X., Delire, C., Koven, C., MacDougall, A., Peng, S., Rinke, A., Saito, K., Zhang, W., Alkama, R., Bohn, T. J., Ciais, P., Decharme, B., Gouttevin, I., Hajima, T., Hayes, D. J., Huang, K., Ji, D., Krinner, G., Lettenmaier, D. P., Miller, P. A., Moore, J. C., Smith, B., Sueyoshi, T., Shi, Z., Yan, L., Liang, J., Jiang, L., Zhang, Q., and Luo, Y.: Terrestrial ecosystem model performance in simulating productivity and its vulnerability to climate change in the northern permafrost region, Journal of Geophysical Research: Biogeosciences, 122, 430-446, 10.1002/2016JG003384, 2017.

Young, F. J., Radatz, C. A., and Marshall, C. A.: Soil survey of Boone County, Missouri, U.S. . Department of Agriculture, N. R. C. S. (Ed.), 2001.

Zaehle, S., Medlyn, B. E., De Kauwe, M. G., Walker, A. P., Dietze, M. C., Hickler, T., Luo, Y. Q., Wang, Y. P., El-Masri, B., Thornton, P., Jain, A., Wang, S. S., Warlind, D., Weng, E. S., Parton, W., Iversen, C. M., Gallet-Budynek, A., McCarthy, H., Finzi, A. C., Hanson, P. J., Prentice, I. C., Oren, R., and Norby, R. J.: Evaluation of 11 terrestrial carbon-nitrogen cycle models against observations from two temperate Free-Air CO2 Enrichment studies, New Phytologist, 202, 803-822, 2014.